

Periodic orbit asymptotics for intermittent Hamiltonian systems

Per Dahlqvist

Mechanics Department

Royal Institute of Technology, S-100 44 Stockholm, Sweden

Abstract - We address the problems in applying cycle expansions to bound chaotic systems, caused by e.g. intermittency and incompleteness of the symbolic dynamics. We discuss zeta functions associated with weighted evolution operators and in particular a one-parameter family of weights relevant for the calculation of classical resonance spectra, semiclassical spectra and topological entropy. For bound intermittent system we discuss an approximation of the zeta function in terms of probabilities rather than cycle instabilities. This approximation provides a generalization of the fundamental part of a cycle expansion for a finite subshift symbolic dynamics. This approach is particularly suitable for determining asymptotic properties of periodic orbits which are essential for scrutinizing the semiclassical limit of Gutzwiller's semiclassical trace formula. The Sinai billiard is used as model system. In particular we develop a crude approximation of the semiclassical zeta function which turns out to possess non analytical features. We also discuss the contribution to the semiclassical level density from the neutral orbits. Finally we discuss implications of our findings for the spectral form factor and compute the asymptotic behaviour of the spectral rigidity. The result is found to be consistent with exact quantum mechanical calculations.

1 Introduction - Dilemmas in Quantum Chaology

There is no definition of *Quantum Chaology* or *Quantum Chaos* which is generally agreed upon. One may focus on the correspondence principle and state the question *How is chaos revealed in a quantum system when the Planck's constant $\hbar \rightarrow 0$, if its classical counterpart is chaotic.* The answer turns out to as complicated as the question is interesting. It seems as if one cannot understand properly the transition from quantum to classical mechanics for a system with few degrees of freedom without considering its coupling to the environment. This coupling may induce decoherence, enabling quasi classical behaviour [1].

One may also (and we will) focus on the more modest question: *What is the behaviour of a quantum system if its classical counterpart is chaotic?* We thus avoid any discussion of decoherence phenomena. Restricting our attention to bounded autonomous systems we may

¹Proceedings of the Los Alamos Center for Nonlinear Science *Quantum Complexity in Mesoscopic Systems*, May 1994, to appear in *Physica D*.

choose e.g. to study quantum spectra. There has been a lot of numerical and experimental studies of the statistical properties of quantum spectra of classically chaotic systems. There are some widely known conjectures inspired by random matrix theories [2]. Although some of the numeric evidence is rather striking there is very little theoretical understanding. Such an attempt naturally starts from the semiclassical trace formula. This formula relates the density of eigen-energies to dynamical invariants of the periodic orbits of a system [3]:

$$g(E) = g_o(E) + \frac{1}{i\hbar} \sum_p T_p \sum_{n=1}^{\infty} \frac{1}{|M_p^n - I|^{\frac{1}{2}}} e^{in[S_p/\hbar - \mu_p \frac{\pi}{2}]} . \quad (1)$$

Here $g(E) = \text{Tr} G(q, q'; E)$ is the trace of the semiclassical Green's function, and the density of eigenstates is given by $d(E) = -\frac{1}{\pi} \lim_{\epsilon \rightarrow 0} \text{Im} g(E + i\epsilon)$. The index p labels the primitive periodic orbits, S_p is the action integral along the orbit, T_p its period, M_p is the linearized Poincaré map around the orbit (monodromy matrix), μ_p is the Maslov index, and $g_o(E)$ provides the mean level distribution. We will exclusively consider billiards and put $\hbar = m = 1$. The semiclassical limit $\hbar \rightarrow 0$ is thus replaced by $E \rightarrow \infty$. The action is given by $S_p = l_p \cdot \kappa(E)$ where κ is the momentum $\kappa = \sqrt{2E}$, and l_p is the length of the prime orbit.

The trace formula is derived through a stationary phase approximation, except for $g_o(E)$ which is calculated from the short time behaviour of the semiclassical propagator. In principle $g_o(E)$ is given by an asymptotic expansion whose leading term is the Weyl term. The division into a mean contribution and an oscillating may turn out to be more involved than anticipated. We will indeed encounter such problems in this paper.

It is often more convenient to study the Gutzwiller-Voros zeta function [4] which for systems with two degrees of freedom reads

$$Z_{GV}(E) = \prod_p \prod_{m=0}^{\infty} \left(1 - \frac{e^{il_p \kappa(E) - \mu_p \frac{\pi}{2}}}{|\Lambda_p|^{1/2} \Lambda_p^m} \right) . \quad (2)$$

where Λ_p is the expanding eigenvalue of M_p . Z_{GV} is related to the level density by

$$g(E) - g_o(E) = \frac{d}{dE} \ln Z(E) , \quad (3)$$

so the zeros of the zeta function are the poles of the of eq. (1), i.e. the semiclassical eigenvalues.

It is not known whether the trace formula manages to give the right density of states on, or close to the real energy axis. Whatever method one uses, only a moderate number of zeros can be computed from a reasonable number of periodic orbits. The exponential proliferation of periodic orbits makes every step towards the semiclassical limit very expensive. It therefore seems impossible in practice to study the semiclassical limit of the semiclassical trace formula by explicit computation of the periodic orbits.

This motivates a study of asymptotic measures of the set of periodic orbits for bound systems, which is the main problem to be addressed in this talk.

We will make extensive use of the concept of *zeta functions*. The most succesful use of zeta functions has been achieved for so called Axiom-A systems (a very strong definition of chaos suitable for making mathematical theorems). Then there are theorems about entireness of the certain classes of zeta functions. However, bounded systems are generally not Axiom-A, they are generally intermittent and lack a simple symbolic dynamics, so practical applications of the theory of zeta functions are not very successful. Since our main motivation is to understand fluctuations in the spectra of bound systems we are presented with another dilemma. It will however turn out that we can make use of this inconvenient intermittent property to formulate approximate zeta functions.

2 A menagerie of zeta functions

This exposition of zeta functions and the thermodynamic formalism is rather brief. The reader may found more details in refs [5, 6, 7, 8, 9] and references therein.

2.1 Evolution operators, trace formulas and zeta functions

Zeta functions are introduced by considering the evolution operator \mathcal{L}_w^t . It describes the evolution of a phase space density $\Phi(x)$

$$\mathcal{L}_w^t \Phi(x) = \int w(x, t) \delta(x - f^t(y)) \Phi(y) dy \quad . \quad (4)$$

The phase space point x is taken by the flow to $f^t(x)$ during time t . $w(x, t)$ is a weight associated with a trajectory starting at x and evolved during time t . It is multiplicative along the flow, that is $w(x, t_1 + t_2) = w(x, t_1) w(f^{t_1}(x), t_2)$. This ensures that the eigenvalues are on the form λ_α^t .

As we are only studying billiards it is convenient to use the length traversed l as *time* variable.

We now compute the trace of the evolution operator, that is, the sum of its eigenvalues $tr \mathcal{L}_w^l = \sum_\alpha e^{ik_\alpha l}$. The trace may be written as a sum over the periodic orbits in the system

$$\begin{aligned} tr \mathcal{L}_w^l &= \int w(x, t) \delta(x - f^l(x)) dx = \\ &= \sum_p l_p \sum_{n=1}^{\infty} w_p^n \frac{\delta(l - nl_p)}{|\det(1 - M_p^n)|} \quad , \end{aligned} \quad (5)$$

The trace may also be written as the Fourier transform of the logarithmic derivative of a *zeta function*

$$tr \mathcal{L}_w^l = \frac{1}{2\pi i} \int_{-\infty}^{\infty} e^{ikl} \frac{Z'_w(k)}{Z_w(k)} dk \quad . \quad (6)$$

The zeta function reads

$$Z_w(k) = \prod_p \prod_{m=0}^{\infty} \left(1 - w_p \frac{e^{-ikl_p}}{|\Lambda_p| \Lambda_p^m} \right)^{m+1} \quad , \quad (7)$$

The k_α 's introduced above should be the zeros of the zeta function. For the system we are going to consider things will be complicated and the operator will not have a discrete spectrum.

By using different weights w one can probe different properties of the flow. We will consider the one-parameter family of weights $\omega = |\Lambda(x, t)|^\tau$. $\Lambda(x, t)$ is the expanding eigenvalue of the Jacobian transverse to the flow. It is only approximately multiplicative along the flow but it is possible to modify it slightly so as to become exactly multiplicative [10]. However, this is a subtlety compared to the approximations we are going to apply.

The leading zero will generally be on the imaginary axis $k = -ih(\tau)$, where $h(\tau)$ are generalized entropies, in the thermodynamic formalism they are usually named *topological pressures*, [11].

Putting $\tau = 0$ we obtain the *classical* zeta function whose zeros yields the so called *resonance spectrum* or spectrum of correlation exponents (again things are complicated if the spectrum is not discrete)

$$Z(k) = \prod_p \prod_{m=0}^{\infty} \left(1 - \frac{e^{-ikl_p}}{|\Lambda_p| \Lambda_p^m} \right)^{m+1} \quad . \quad (8)$$

The leading zero provides the escape rate. For a bound system the escape rate equals zero: $h(0) = 0$.

The *topological* zeta function is obtained by considering the case $\tau = 1$. The leading zero now gives the topological entropy $h(1)$. The asymptotic behaviour of the trace is

$$tr \mathcal{L}_{top}^l \approx \sum_p l_p \sum_{n=1}^{\infty} \delta(l - nl_p) \rightarrow e^{h(1)t} \quad (9)$$

so that the number of cycles with periods less than l is $\sim e^{h(1)l}/h(1)l$. To obtain this exponential increase, the contour of the Fourier transform (6) must extend below all zeros where the Euler product (7) converges.

Let us now study the case $\tau = 1/2$. We then get

$$Z_{sc}(k) = \prod_p \prod_{m=0}^{\infty} \left(1 - \frac{e^{-ikl_p}}{\sqrt{|\Lambda_p|} \Lambda_p^m} \right)^{m+1}. \quad (10)$$

This zeta function is called *the quantum Fredholm determinant* [6, 7] and is equivalent to the Gutzwiller-Voros zeta function in the semiclassical limit through the identification $\kappa(E) = -k$. Its leading zero is closer to the origin than the topological one $0 < h(1/2) < h(1)$, cf. sections 2.2 and 3.3. This zero provides a pole in the trace formula, and the periodic orbit sum (5) as well as the trace formula (1) diverge in the half plane above it. This is usually referred to as an entropy barrier. The Euler-product representation of the zeta function (7) also diverges above this leading zero (because the zero is not a zero of an individual factor and an infinite product is not allowed to converge towards zero). We have left out the Maslov indices but it is possible to account for them in the weight as well. The introduction of phase indices will shift the the leading zero towards the origin as we soon will see.

2.2 Cycle expansions of zeta functions

The zeta functions have been formulated as Euler products. These products diverge wherever they are interesting (i.e. at the nontrivial zeros). In computations, one generally expands them into infinite series, power series in the case of maps and Dirichlet series in case of flows. Power series converge up to its first singularity and are thus better for computations. Dirichlet series are more complicated, they may have a strip of conditional convergence and do not necessarily have singularities on its border(s) of convergence.

Zeta functions are entire if the system has a Poincaré map which is analytic, hyperbolic and have a finite subshift symbolic dynamics [12]. In that case the expansion may be divided into a fundamental part, yielding the gross structure of the spectrum, and *curvature corrections* [8]. The standard example is the expansion of the *dynamical zeta function* (i.e. the $m = 0$ factor of the zeta functions above) for a system with binary symbolic dynamics:

$$\begin{aligned} \prod_p (1 - t_p) = & \\ 1 - t_1 - t_0 & \\ -[t_{10} - t_1 t_0] & \\ -[t_{100} - t_{10} t_0] - [t_{110} - t_1 t_{10}] & \\ -[t_{1100} - t_1 t_{100} - t_{110} t_0 + t_1 t_{10} t_0] - [t_{1110} - t_1 t_{110}] - [t_{1000} - t_{100} t_0] & \\ - \dots & \end{aligned} \quad (11)$$

where $t_p = \exp(-il_p k)/|\Lambda_p|^{1-\tau}$. The expansion is organized according to increasing symbol length in an obvious way, in the case of a map (the l_p 's being integers) this means according to increasing powers of $\exp(-ik)$. The expansion is dominated by the *fundamental* contribution, $1 - t_1 - t_0$. For the lowest powers there is a nice interpretation why the rest of the expansion is small [8]. The tail of the expansion is organized in such a way that each square bracket contains some long orbit(s) (length n) minus its approximant(s) in terms of shorter ones. The sizes of these *curvature corrections* fall off exponentially with n . This leads to a pole lying beyond the leading zero. Similar expansion for the full zeta function has infinite radius of convergence (under the above conditions) such that nonleading zeros may be extracted.

Example. Let us consider a hypothetical billiard having the Baker's map as Poincaré map. Then $|\Lambda_p| = 2^{n_p}$. Let further the periods be discretized $T_p = n_p T_0$. Only the fundamental part will remain:

$$Z = 1 - 2 \frac{e^{T_0 k}}{2^{1-\tau}} \quad (12)$$

with leading zero $= -i\tau \log 2/T_0$. We see that $h(0) = 0$ as it should be for a bound system and the topological entropy is $h(1) = \log 2/T_0$. This is of course a very unrealistic example and the semiclassical spectrum, $\tau = 1/2$, does not look sensible at all.

If the symbolic dynamics is a more general, finite subshift (meaning that there is a *finite* set of *pruning rules*), this scheme may still be worked out. There is a wealth of illustrative examples in ref. [8]. However, if the symbolic dynamics is not a finite subshift there will be no similar expansion. The scheme outlined here is therefore not applicable for a generic bound system. In this case there is not even a well defined fundamental part. We will suggest a solution of this dilemma in the next section.

2.3 Zeta functions in the BER approximation

In ref. [9] an approximate expression for the zeta function is given for intermittent, ergodic Hamiltonian systems. The idea is based on a paper by Baladi, Eckmann and Ruelle [13] so we refer to it as the BER approximation.

In an intermittent system laminar intervals are interrupted by chaotic outbursts. Let Δ_i be the time elapsed between two successive entries into the laminar phase. The index i labels the i 'th interval. Provided the chaotic phase is *chaotic enough*, the lengths of the intervals Δ_i are presumed uncorrelated, and Δ may be considered as a stochastic variable with probability distribution $p(\Delta)$. The zeta functions may then be expressed in terms of the Fourier transform of $p(\Delta)$

$$Z(k) \approx \hat{Z}(k) \equiv 1 - \int_0^\infty e^{-ik\Delta} p(\Delta) d\Delta \quad (13)$$

We use the "ˆ" symbol to mark all quantities derived in the BER approximation.

3 The Sinai billiard - Classical considerations

The Sinai billiard [14] consists of a unit square with a scattering disk, having radius R ; $0 < 2R \leq 1$, centered on its midpoint. This billiard has a fairly simple geometry, but exhibits many features typical for bound chaotic system; it is intermittent and lacks a simple symbolic dynamics.

The trajectory of a particle in the Sinai billiard consists of laminar intervals, (bouncing between the straight sections) interrupted by scatterings off the central disk. The Sinai billiard seems therefore suited for the BER approximation. The variable Δ introduced above is simply the length of the trajectory segment between two disk bounces.

The material of this section, except for sect. 3.3, is developed in ref [15] in more detail.

3.1 Formulation of $p(\Delta)$ and a generalization

We use the disk to define the surface of section. The canonical variables are $(R\phi, \sqrt{2E} \sin \alpha)$ with the angles $0 < \phi \leq 2\pi$ and $-\frac{\pi}{2} < \alpha < \frac{\pi}{2}$ defined in fig. 1a. The map $(\phi, \sin \alpha) \mapsto (\phi, \sin \alpha)$ is area preserving and has uniform invariant density.

We will now use this uniformity to formulate an expression for $p(\Delta)$. To that end we use a natural partition of the surface of section defined by the topology of the problem. Suppose a laminar segment hits the vertical walls n_x times, and the horizontal walls n_y times. Equivalently one can unfold the billiard into a regular lattice of disks. These disks are assigned numbers $q = (n_x, n_y)$, as in fig 1b. Only one octant need to be considered due to the C_{4v} symmetry, so we take n_x and n_y positive, and $n_x \geq n_y$. The segment under study starts out from $q = (0, 0)$. It is obvious that only coprime $q = (n_x, n_y)$ can be reached. Now let Ω_q be the part of phase space (ϕ, α) for which the trajectory hit disk q . Let us make the further approximation that all trajectories going from $(0, 0)$ to q have the same length l_q . We then get the following approximation for $p(\Delta)$

$$\hat{p}(\Delta) \approx \sum_q a_q(0) \delta(\Delta - l_q) \quad , \quad (14)$$

Figure 1: a) The Sinai billiard with definitions of of the phase space variables ϕ and α .
b) The unfolded system with free directions (corridors) indicated.

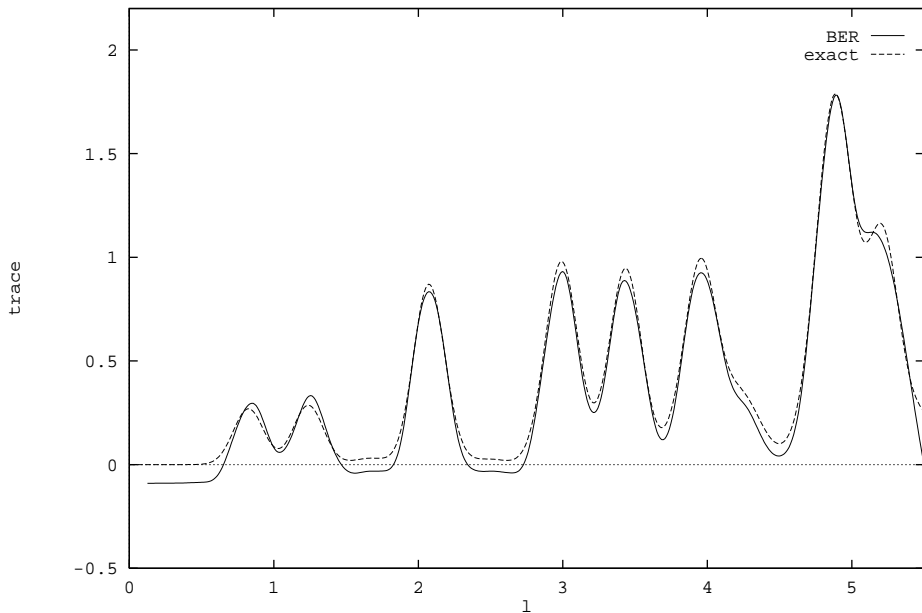


Figure 2: The trace of the evolution operator (unit weight, $\tau = 0$) for the BER approximation and the explicit periodic orbit sum. Both curves has been smoothed by a gaussian having width $\sigma = 0.1$. The disk radius is $R = 0.1$. From [15].

where $a_q(0)$ is given by

$$a_q(0) = \frac{2}{\pi} \int_{\Omega_q} d\phi d(\sin \alpha) . \quad (15)$$

This approach is not restricted to the $\tau = 0$ case. To treat the other cases we simply average a power of the local instability $|\Lambda(\phi, \alpha)| \approx \frac{2l_q}{R \cos(\alpha)}$ over Ω_q . This leads to the generalized probability distributions

$$\hat{p}_\tau(\Delta) \approx \sum_q a_q(\tau) \delta(\Delta - l_q) , \quad (16)$$

with

$$a_q(\tau) = \frac{2}{\pi} \int_{\Omega_s} |\Lambda(\phi, \alpha)|^\tau d\phi d(\sin \alpha) \quad (17)$$

The zeta function may now be written

$$\hat{Z}_\tau(k) = 1 - \int_0^\infty e^{-ik\Delta} \hat{p}_\tau(\Delta) d\Delta \approx 1 - \sum_q a_q(\tau) e^{-ikl_q} , \quad (18)$$

3.2 Comparison with periodic orbit calculations

The formulation of $\hat{p}_\tau(\Delta)$ can be further refined. The region Ω_q may divided into eight parts Ω_s with $s = (g, q)$ where g depend on the octant from which the trajectory has arrived. This eight octants correspond to the eight elements of the symmetry group $g \in C_{4v}$ of the billiard. The zeta function now reads

$$\hat{Z}_\tau(k) \approx 1 - \sum_s a_s(\tau) e^{-ikl_s} , \quad (19)$$

This amounts to restricting the system to the fundamental domain and study one symmetry subspace A_1 of the original problem, see refs. [15, 16]. For each Ω_s there is an orbit \bar{s} periodic in

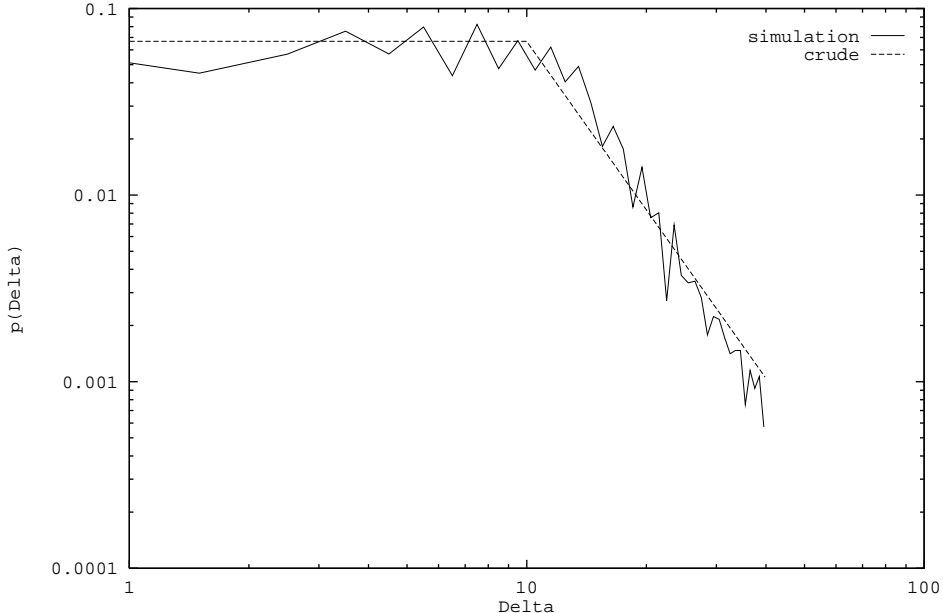


Figure 3: $p(\Delta)$ from numerical simulation, compared with the crude approximation of sect 3.3. The disk radius is $R = 0.05$.

the fundamental domain. We choose l_s to be the length of this orbit. (It may need to go through an intermediate disk, but l_s is well defined irrespective if \bar{s} is pruned or not). Other subspaces may also be considered by inserting group characters, see [15, 16]. We will not discuss them here to keep things as simple as possible.

At this point it is interesting to check if this approximate zeta function can reproduce the exact trace by means of the periodic orbit sum (5), see fig 2. This plot, reaching up to $l = 5.5$, involves ~ 8000 periodic orbits. The exponential proliferation of cycles means that we cannot go very much higher in l by explicit periodic orbit calculations. The conclusion so far is that the BER approximation gives a very good description, which is generally improved for larger l , see ref. [15]. The fine scale structure can of course not be reproduced due to the introduction of deltafunctions in section 3.1 and due to the BER approximation itself. The topological zeta function ($\tau = 1$) was examined in ref. [15], also with good results. It is also demonstrated in ref [15] that the exact topological zeta function is obtained in the limit $R \rightarrow 0$. The conclusion is that the method works for any value of τ .

3.3 A crude approximations to $p_\tau(\Delta)$

We will now work out a very crude approximation to $p_\tau(\Delta)$ which will turn out to be both illustrative and useful. For any disk radius $0 < R < 1/2$ there is a finite number of directions along which a trajectory may go without ever bouncing off a disk (see fig 1b)! We call them *free directions*, or *corridors*. Consider the direction vector (x, y) . A direction cannot be free if x/y is irrational. So we may take (x, y) as positive coprime integers (n_x, n_y) such that $n_x/n_y \leq 1$. It is a little confusing that (n_x, n_y) may refer both to a particular disk in the unfolded system and a corridor but thus ambiguity will turn out to be rather convenient. The direction (n_x, n_y) is free if [15, 17]

$$2R < \frac{1}{\sqrt{n_x^2 + n_y^2}} \quad . \quad (20)$$

This means that if disk $q = (n_x, n_y)$ lies inside radius $1/2R$ there are no obstructing disks in front of it, see fig 1b. Next we assume that the disk radius is small and set $l_q = \sqrt{n_x^2 + n_y^2}$. The integral (17) for $l_q < 1/2R$ is trivial

$$a_q(\tau) \approx \frac{2}{\pi} \frac{\Gamma(\frac{2-\tau}{2})^2}{\Gamma(2-\tau)} \left(\frac{R}{l_q}\right)^{1-\tau} . \quad (21)$$

In order to find an approximate expression for $p_\tau(\Delta)$ we must know the density of coprime lattice points with respect to the radius in the first octant $d_c(r)$. This is, to leading order, found to be $d_c(r) \approx \frac{2\pi}{13}r$, see Appendix and fig 6. This yields

$$p_\tau(\Delta) = \sum_q \delta(\Delta - l_q) a_q(\tau) = d_c(\Delta) \cdot a_q(\tau)|_{l_q=\Delta} = \frac{16}{13} \frac{\Gamma(\frac{2-\tau}{2})^2}{\Gamma(2-\tau)} R^{1-\tau} \Delta^\tau . \quad (22)$$

Obviously the disk radius has to be small for this to apply.

If $\Delta \geq 1/2R$ the disks start to obscure each other. The accessible disks are those along the corridors, see fig 1b. They may be written on the form $q_n = q' + n \cdot q''$. Here, $q'' = (n_x'', n_y'')$ is a free direction and q' is one of its neighbours in the Farey sequence of order n_x'' [18]. The a_q 's decrease as [15]

$$a_q(\tau) \sim \frac{1}{n^{3-3\tau/2}} \quad (23)$$

and the corresponding lengths grow linearly

$$l_{q_n} \approx \text{const} + n \cdot q_{free} \quad (24)$$

The last two equations imply that

$$p_\tau(\Delta) \sim \frac{1}{\Delta^{3-3\tau/2}} \quad \Delta \gg \frac{1}{2R} \quad (25)$$

Of course, there is a transition region around $\Delta \sim 1/2R$ but if we accept a kink at $\Delta = 1/2R$ and require $p_\tau(\Delta)$ to be continuous we obtain

$$p_\tau(\Delta) \approx p_\tau^{crude}(\Delta) = \begin{cases} \frac{4}{3} \frac{\Gamma(\frac{2-\tau}{2})^2}{\Gamma(2-\tau)} R^{1-\tau} \Delta^\tau & \Delta \leq 1/2R \\ \frac{4}{3} \frac{\Gamma(\frac{2-\tau}{2})^2}{\Gamma(2-\tau)} \frac{2^{\tau/2-3} R^{-\tau/2-2}}{\Delta^{3-3\tau/2}} & \Delta > 1/2R \end{cases} \quad (26)$$

We have multiplied the prefactors with a factor $13/12$ so that $Z_{\tau=0}^{crude}(0) = 0$, our approximations otherwise violate the normalization of $p(\Delta)$. In fig. 3 we compare this expression with a numerical simulation of the billiard for the case $\tau = 0$. Our crude approximation is a good smoothed approximation to $p(\Delta)$.

The most obvious length scale in the Sinai billiard is the length of the shortest periodic orbit $l_0 \approx 1$. We have now learned that there is another important length scale, $l_{scale} = 1/2R$, given by the kink above, being the mean free path in the unfolded system. We will subsequently understand that this is a very important length scale even for the quantum problem.

A crude estimation of the zeta function $Z_\tau^{crude}(k)$ is obtained by a Fourier transform of $p_\tau^{crude}(\Delta)$. What can we say about its analytic structure?

The leading zero $k_0 = -ih(\tau)$ as obtained from this zeta function is plotted versus τ for two different disk radii in fig. 4. We see that the behaviour is not at all linear as was the case in the example of section 2.2, which is the case only for uniformly hyperbolic systems. The Sinai billiard is anything but uniformly hyperbolic, the intermittency becomes more and more pronounced as R decreases and the deviation from a linear function increases accordingly. Note that a linear dependence is often assumed in some oversimplified (erroneous) estimations of the *entropy barrier* in the literature.

For small τ , that is, when the zero is close to the origin, the zeta function is dominated by the large l tails. Further away from the origin it is dominated by the closest disk. The topological

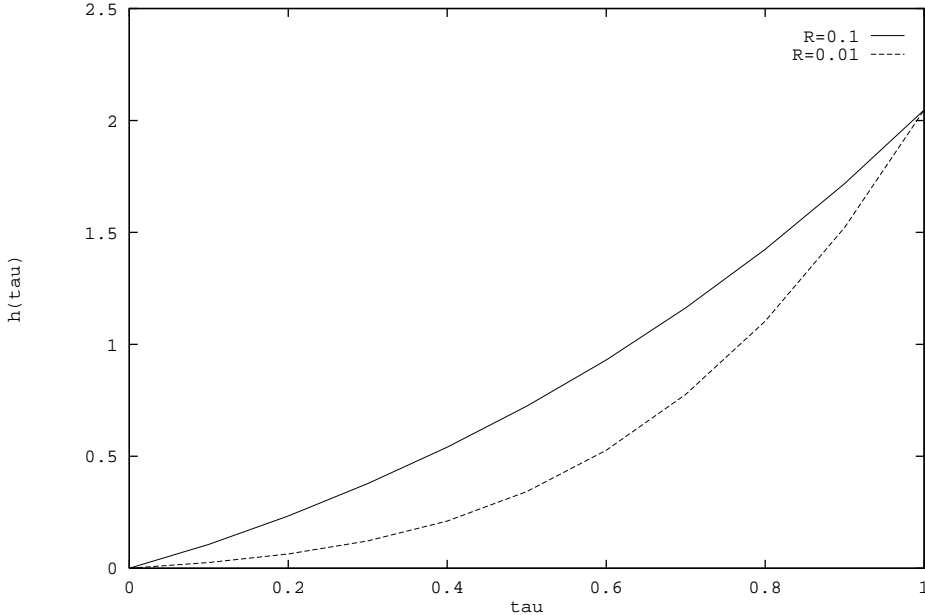


Figure 4: The generalized entropies $h(\tau)$ as given by the leading zero of the crude approximation of the zeta function.

entropy $h(1)$ obtained this way is 5% wrong in the limit $R \rightarrow 0$, see ref. [15]. The reason is twofold: the ad hoc renormalization of the prefactor, and secondly, for this large τ the value is dominated by the closest disks.

Equipped with our crude estimation of the zeta function we can insert it onto (6) and compare the trace obtained with the result of section 3.2. The comparison is made in fig. 5. We see that the crude approximation give a good average description. We see that when $l > l_{scale}$ the curve starts to approach an asymptotic behaviour. What is this limiting behaviour.

The power law tail of $p_\tau(\Delta)$ introduces a branch cut of the zeta function along the positive imaginary axis. The asymptotics of the Fourier transform (6) is governed by this cut. Let us be slightly more general and consider an arbitrary (generalized) distribution $p_\tau(\Delta)$ with a power law tail $\sim 1/\Delta^m$. Then an elementary calculation yields

$$\frac{1}{2\pi i} \int_{-\infty}^{\infty} e^{ikl} \frac{Z'_w(k)}{Z_w(k)} dk \sim \begin{cases} 1 - \frac{p_\tau(\Delta_0)\Delta_0^m}{(m-1) \int \Delta p_\tau(\Delta) d\Delta} \frac{1}{l^{m-2}} & Z(0) = 0 \quad m > 2 \\ -\frac{p_\tau(\Delta_0)\Delta_0^m}{\int p_\tau(\Delta) d\Delta} \frac{1}{l^{m-1}} & Z(0) \neq 0 \quad m > 1 \end{cases} \quad (27)$$

Δ_0 is any point in the tail of $p_\tau(\Delta)$. The results are valid also for non integer m . To obtain these results we let the contour of the Fourier integral run along the real axis. To get consistency with the explicit periodic orbit sums (5) for $\tau > 0$ one has to extend the integration below all the zeros which will pick up up exponentially increasing terms.

Note that there will be a sudden change in the asymptotic behaviour when $\tau = 0$. One say that a phase transition occurs at this point; the exponential behaviour of the trace is taken over by a power law. When $\tau = 0$ the cut reaches down to the leading zero preventing exponential mixing.

3.4 Relation to cycle expansions

All values of the symbol $s = (q, g)$ (introduced in section 3.2 and corresponding to one laminar segment) can be realized if q lies within the horizon. An idea is now to build strings of these

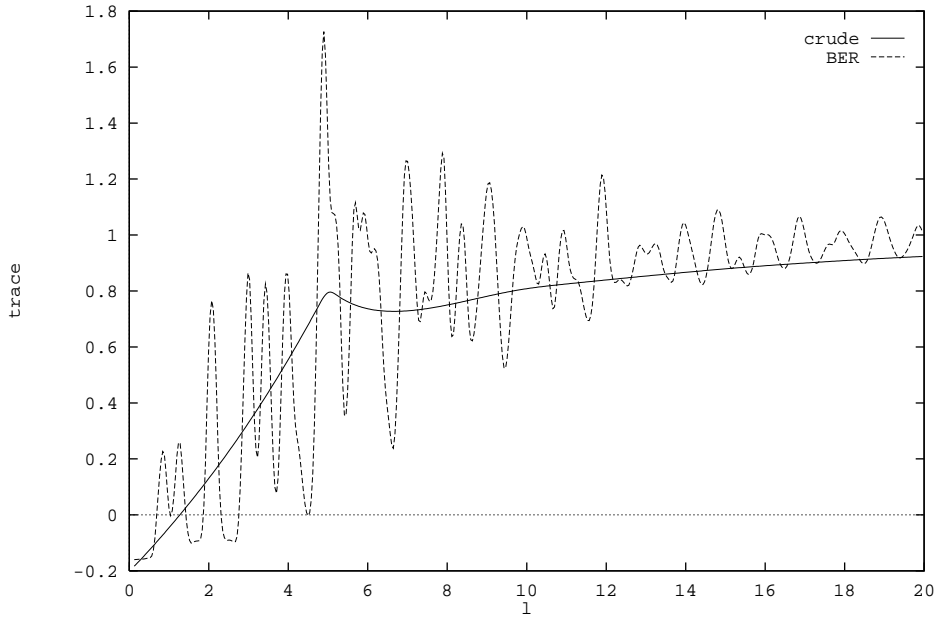


Figure 5: The trace of the evolution operator ($\tau = 0$), calculated from the crude approximation (sect. 3.3) and the more refined approximations (sect. 3.2) of the zeta functions, for disk radius $R = 0.1$.

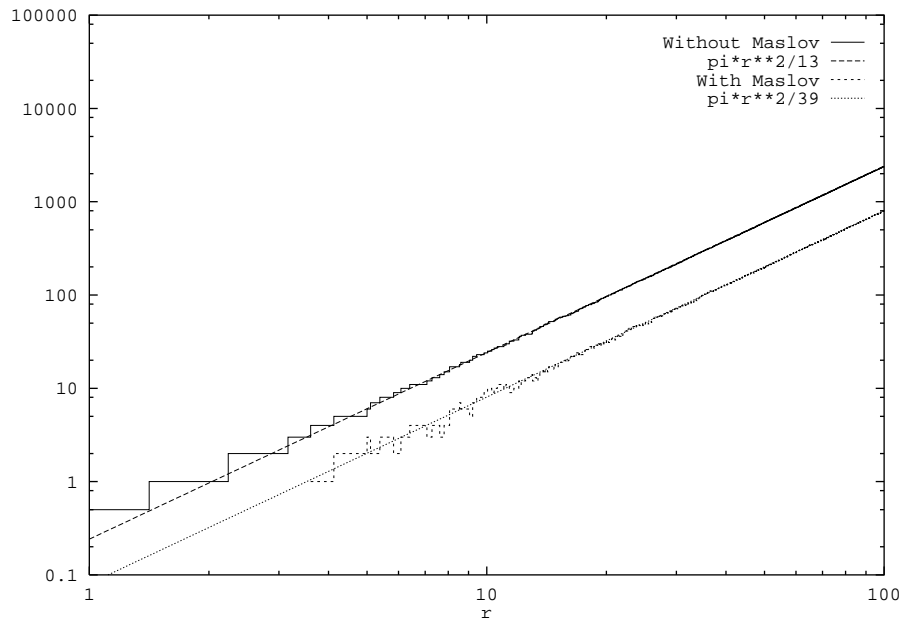


Figure 6: The number of coprime lattice point, with and without *Maslov weights*, inside radius r , compared with the asymptotic results obtained in the Appendix.

symbols and build up arbitrary trajectories $s_1 s_2 s_3 \dots$ and so define a symbolic dynamics. If all the s 's lies inside the horizon almost all such sequences could be realized and the symbolic dynamics would be almost complete. This would yield a fundamental part of a cycle expansion

$$Z(k) = 1 - \sum_s \frac{1}{|\Lambda_s|^{1-\tau}} e^{-ikl_s} . \quad (28)$$

If we compare this expression with eq (18) together with eq (21) we see an apparent similarity. Indeed the prefactors are almost the same, see [15]. (To make this comparison one first writes the sum $\sum_{s=(q,g)} = \sum_q \sum_g$ and sums over g .)

The cycle expansion breaks down when some of the s 's are outside the horizon whereas the BER approximation works fine. The conclusion is that the approximation worked out in sections 3.1 to 3.3 provides a good generalization for the fundamental part of a cycle expansion. Indeed it is both better (it automatically preserves unitarity) and simpler as it does not use an enormous amount of periodic orbits to explore the available phase space for one single symbol but rather measure it directly. Neither does it need all these cycles in order to find out that the invariant density is uniform as we already knew that in advance.

4 The Sinai billiard - Semiclassical considerations

For the quantum Sinai billiard a major part is played by the (one parameter families) of neutral periodic orbits. The level density can be written as a sum of the mean density and two oscillating parts, one from the unstable orbits (expressed by the Gutzwiller formula) and one due to neutral orbits.

$$d(E) \equiv \sum_\nu \delta(E - E_\nu) = \bar{d}(E) + d_u^{osc}(E) + d_n^{osc}(E). \quad (29)$$

The semiclassical approximation can be refined by taking creeping orbits [19] and ghost orbits [20] into account, but we neglect them here. We will now discuss the two oscillating contributions separately. In the discussion of the contribution from unstable orbits we will focus on convergence and singularities of the zeta function. The considerations for neutral orbits are worked out for use in section 5.

4.1 The contribution $d_u^{osc}(E)$ from unstable orbits

We use the BER approximation to approximate the Gutzwiller-Voros zeta function and we will use the rough approximations of section 3.3, putting $\tau = 1/2$, and $\kappa = \sqrt{2E} = -k$. According to our previous investigations we now expect this zeta function to approximate the Gutzwiller-Voros zeta function for small k , well below the first quantum state. This is certainly not the semiclassical limit but will lead to some interesting observations.

We now have to introduce Maslov indices. The generalization of p_τ now includes an oscillating weight (we still restrict us to the A_1 subspace):

$$\tilde{p}_{1/2}(\Delta) \approx \sum_{q=(n_x, n_y)} (-1)^{n_x + n_y + 1} a_q(\tau) \delta(\Delta - l_q) . \quad (30)$$

The $a_q(\tau)$'s are the same as before but the definition of the generalized density of coprimes $\tilde{d}_c(r)$ must now include the oscillating weight. The result appears to be exactly one third of the previous result $\tilde{d}_c \sim \frac{2\pi}{39} r^2$, see Appendix and fig 6. The crude approximation of the probability distribution is obtained by simply multiplying eq. (26) by one third.

The zeta function is obtained by Fourier transforming our approximation of $\tilde{p}_{1/2}(\Delta)$. An interesting question is if its leading zero is still below the real k axis. In this approximation it follows from (26) (with the extra factor of one third) that this is the case if

$$R < \frac{44 \Gamma(3/4)^2}{135 \sqrt{2} \Gamma(3/2)} \approx 0.3905 \quad (31)$$

For radius as big as the limiting value the approximation has already ceased to be relevant. We must expect that the Euler product (2) is divergent on the real axis and in a strip below, but the leading zero can be very close to the real axis. It may very well happen that the zero crosses the real axis for other subspaces.

If there is a zero below the real axis it will mean that the Gutzwiller trace formula diverges on the real axis. In that case, whenever we encounter a periodic orbit sum like (5) it must be regularized. This amounts to keep the contour of the Fourier integral along the real axis. As all our approximate zeta functions converges in the entire lower halfplane this is not a major problem.

It is interesting to compare this situation with the Selberg zeta function for systems with constant negative curvature. Along the real $k(= -\kappa)$ axis the Selberg zeta function has zeros on the exact (quantum) locations, which is a peculiarity of these systems. In addition it has a leading zero on the negative imaginary axis, in exact analogy with our crude estimations of the zeta functions for the Sinai billiard. The situation is similar for the Riemann zeta function.

Our semiclassical zeta function has a cut along the positive imaginary axis (and an infinite number of parallel cuts, cf. ref. [15]). Do we allow the semiclassical zeta function to have non analytical features? Well, the semiclassical approximation to the spectral determinant $D(\kappa)$ is $D(\kappa) \approx D_{sc}(\kappa) = \exp(-i\pi(\bar{N} + N_n^{osc}))Z_{GV}(\kappa)$. Its exact quantum counterpart $D(\kappa)$ obeys the functional equation $D(\kappa) = D(-\kappa)$. There is nothing saying a priori that $D_{sc}(\kappa)$ must obey this relation (it would be violated by a cut), it could be an artifact reflecting the shortcomings of the stationary phase approximation and/or the singularity of the semiclassical limit.

But it should be noted that the best semiclassical calculations for chaotic systems so far is obtained by imposing the functional equation to the Gutzwiller-Voros zeta function. It is shown [21] that this requires a remarkable bootstrapping property between short and long periodic orbits. That such a bootstrapping indeed occurs is supported by the results of ref [22]. There are ways of saving the semiclassical determinant from violating the functional equation. The contribution from neutral orbits has cuts at the same places as Z_{GV} but they do not cancel, but the mean staircase $\bar{N}(\kappa)$ could have nonanalyticities cancelling the (main) cut of Z_{GV} and N_n^{osc} . This would extend the bootstrapping ideas mentioned above as \bar{N} is governed by the short time behaviour and the cuts of Z_{GV} by the long periodic orbits. Generally \bar{N} is given by an asymptotic expansion so it shouldn't be surprising if this expansion lead to a cut.

In the classical case the cut carry information about the power law decay of correlations [15]. It would be nice to know what it tells us in the quantum case.

4.2 The contribution $d_n^{osc}(E)$ from neutral orbits

There is a neutral orbit in any free direction. The general formula is [23]

$$d_n^{osc} = \sum^+ 2B_i \cos(\kappa l_i) \quad (32)$$

with

$$B_i = \frac{1}{(2\pi)^{3/2}} \sqrt{\frac{l_p}{|n_i|\kappa}} D_{p_i} \equiv \tilde{B}_i \frac{1}{\sqrt{\kappa}} \quad (33)$$

The index i runs over all neutral periodic orbits. Their length is written as $l_i = n_i l_{p_i}$ where n_i is a repetition number and l_{p_i} the length of the corresponding primitive periodic orbit. D_{p_i} is the geometrical width of the orbit. Note that this contribution is $O(1/E^{1/4})$ whereas the one due to unstable orbits is $O(1/E^{1/2})$. The reason that the unstable orbits still are important is because they are so numerous. Generally the neutral orbits affect the low part of the spectrum and large scale structures in the higher part of the spectrum.

For later purposes it is convenient to sum over both positive and negative traversals

$$d_n^{osc} = \sum^{\pm} B_i e^{i\kappa n_i l_{p_i}} \quad (34)$$

Instead of applying these equations directly it is instructive to first consider the integrable $R \rightarrow 0$ limit of the Sinai billiard. The wavefunction must now vanish at the midpoint which is the relic of the disk. The spectrum is given by $E = 2\pi^2(n^2 + m^2)$ where m, n are positive integers. This leads to a mean level density $\bar{d} = 1/8\pi$ which differs from the Weyl term $\bar{d} = 1/2\pi$. The reason is that is that the $R \rightarrow 0$ is a very odd system quantum mechanically, only having wave functions in two of the symmetry classes (A_2 and B_2).

To find $d_n^{osc}(E)$ we perform the Berry-Tabor trick [24] and rewrite the level density by means of the Poisson's summation formula

$$d_n(E) = \sum_{m,n} \delta(E - 2\pi^2(m^2 + n^2)) = \sum_{M,N=-\infty}^{\infty} \int dn dm \delta(E - 2\pi^2(m^2 + n^2)) e^{2\pi i(Nn + Mm)} \quad (35)$$

Performing the integral by stationary phase we arrive at (32) with

$$\tilde{B}_i = \frac{1}{(2\pi)^{3/2} \sqrt{N^2 + M^2}} \quad (36)$$

and

$$l_i = \sqrt{N^2 + M^2} \quad (37)$$

where i ranges over all pairs (M, N) in the first quadrant. Only one symmetry class (say A_2) is considered if we restrict the summation to the first octant (not bothering how to treat lattice points on the symmetry line $M = N$). If we now write the lattice vector as $(M, N) = n(n_x, n_y)$ where (n_x, n_y) are coprime, we will get consistency with (33) if $l_p = \sqrt{n_x^2 + n_y^2}$ and $D_p = 1/l_p$.

The width D_p decreases as the radius R increases. Inspecting (20) we realize that the width then becomes $D_p = 1/l_p - 2R$. These results are derived in ref. [17] in another way.

With the equipment procured so far we will now attempt to calculate the spectral form factor.

5 More semiclassics - The spectral form factor

A lot of information about spectral fluctuations is encoded in the spectral form factor [25]

$$K(\mathcal{T}) = \frac{1}{\bar{d}} \int_{-\infty}^{\infty} d\epsilon e^{i2\pi\bar{d}\mathcal{T}\epsilon} \langle d^{osc}(E - \frac{\epsilon}{2}) d^{osc}(E + \frac{\epsilon}{2}) \rangle_E \quad (38)$$

The averaging $\langle \dots \rangle_E$ has been performed in a small range ΔE such that $\bar{d}^{-1} \ll \Delta E \ll E$. If there are contributions from both neutral and unstable orbits the form factor divides into three parts (with obvious notations)

$$K(\mathcal{T}) = K_{nn}(\mathcal{T}) + K_{uu}(\mathcal{T}) + K_{un}(\mathcal{T}) \quad (39)$$

The suggested universal form factor relevant for time reversible chaotic systems is that of the Gaussian Orthogonal Ensemble (GOE) which reads [26]

$$K_{GOE} = \begin{cases} 2\mathcal{T} - \tau \log(1 + 2\mathcal{T}) & \mathcal{T} \leq 1 \\ 2 - \mathcal{T} \log \frac{2\mathcal{T}+1}{2\mathcal{T}-1} & \mathcal{T} \geq 1 \end{cases} \quad (40)$$

5.1 The contribution from neutral orbits: $K_{nn}(\mathcal{T})$

If we insert d_n^{osc} into the definition of $K_{nn}(\mathcal{T})$, and expanding $\sqrt{2E + \epsilon} \approx \sqrt{2E} + \epsilon/\sqrt{2E}$ we obtain

$$K_{nn}(\mathcal{T}) = \frac{2\pi}{\bar{d}} \sum_i^{\pm} \sum_j^+ \tilde{B}_i \tilde{B}_j \delta(l - \frac{l_i + l_j}{2}) \langle \cos(\sqrt{2E}(l_i - l_j)) \rangle_E \quad (41)$$

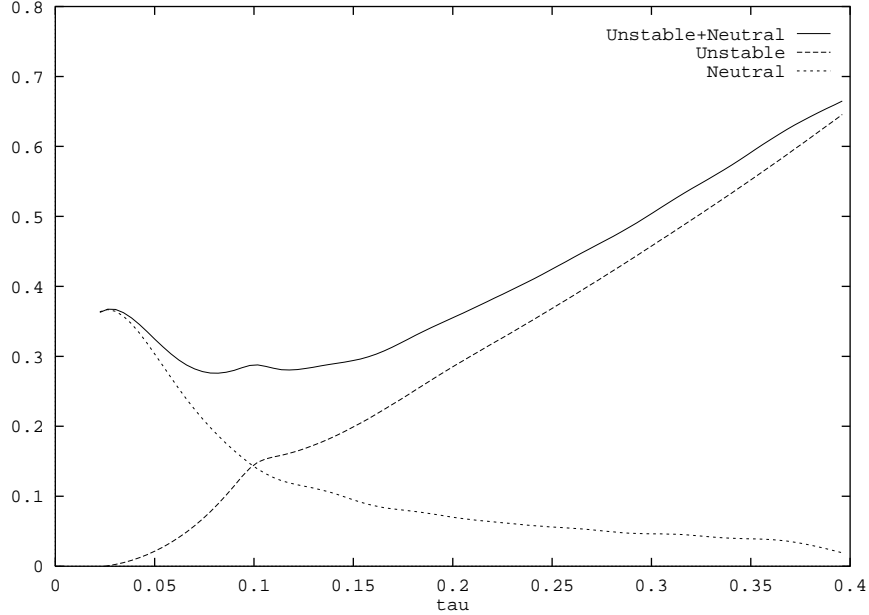


Figure 7: The contributions K_{nn} and K_{uu} and their sum. The latter is calculated from eq (44) using the methods of section 3.3. The parameters are $R = 0.1$ and $\mathcal{T}_{scale} = 0.1$.

where the length variable $l(\mathcal{T}) = \sqrt{2E}2\pi\bar{d}\mathcal{T}$. This expression is always dominated by the diagonal terms [24]

$$K_{nn}(\mathcal{T}) \approx \frac{2\pi}{\bar{d}} \sum_i \tilde{B}_i^2 \delta(l - l_i) . \quad (42)$$

For an integrable system this always equals unity [24]. This can be easily checked for the Sinai $R \rightarrow 0$ billiard by replacing the sum $\sum_{M,N}$ by an integral and using polar coordinates.

If R is very small and l is far from l_{scale} , K_{nn} will still be close to unity, but it will now decrease with increasing \mathcal{T} . An example is given in fig. 7.

Let us now study the case $l \gg l_{scale}$. We can be more general and consider an arbitrary system with a finite number of primitive neutral orbits in the limit $l \gg \max_p l_p (= l_{scale})$ for the Sinai case) we have

$$K_{nn}(\mathcal{T}) = \frac{1}{(2\pi)^2 \bar{d}} \sum_p l_p D_p^2 \sum_n \frac{1}{n} \delta(l - nl_p) = \frac{1}{(2\pi)^2 \bar{d}} \frac{1}{l(\mathcal{T})} \sum_p l_p D_p^2 . \quad (43)$$

We thus have an inverse power law decay, $K_{nn} \sim \frac{1}{\sqrt{E}\mathcal{T}}$ in contradiction to the large \mathcal{T} limit of the GOE prediction $K_{GOE} \sim 1 - \frac{1}{12\mathcal{T}^2}$.

5.2 The contribution from unstable orbits: $K_{uu}(\mathcal{T})$

In the limit $\mathcal{T} \ll 1$ this contribution to the form factor is also dominated by the diagonal terms. However, the result must be multiplied by two [25] since most periodic orbits in time reversible systems are rotations, and each rotation counts as two cycles with exactly the same length. We insert the trace formula into the definition of the form factor and express the result in terms of the trace of the evolution operator

$$K_{uu}(\mathcal{T}) = 2\mathcal{T} \text{tr} \mathcal{L}_{\tau=0}^{l(\mathcal{T})} \quad (44)$$

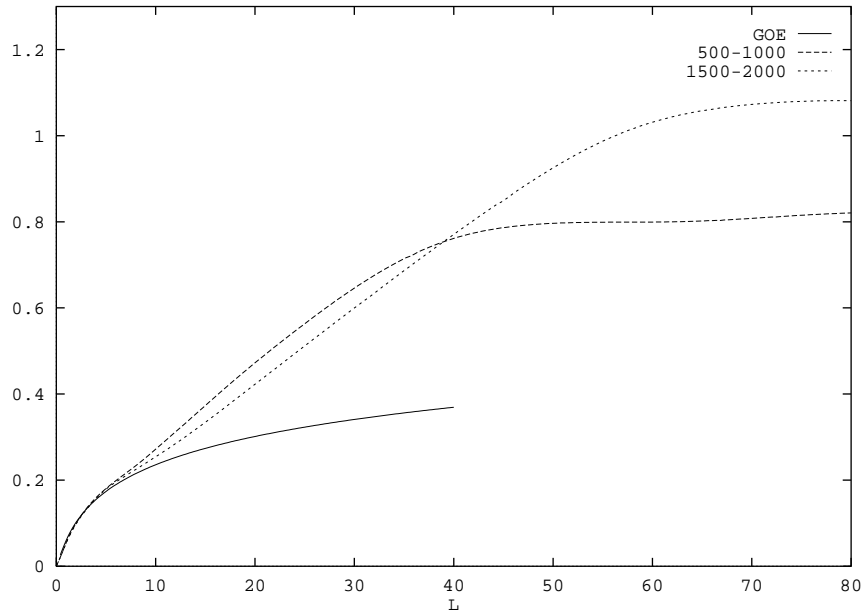


Figure 8: The spectral rigidity of the Sinai billiard calculated from two subsets of the spectrum and compared with GOE. The radius $R = 0.1$. The relevant scale \mathcal{T}_{scale} is slightly above (below) $\mathcal{T}_{scale} = 0.1$ for the lower (higher) part of the spectrum.

An example of this function is found in fig 7. If $\mathcal{T}_{scale} \ll \mathcal{T} \ll 1$ we find, after consulting eqs. (26) and (27), that $K_{uu} = 2\mathcal{T} - 2\mathcal{T}_{scale}$ where the first term agrees with the universal GOE result [25] and the second being a correction dying out in the limit $E \rightarrow \infty$. \mathcal{T}_{scale} is the scale corresponding to l_{scale} given by $\mathcal{T}_{scale} = l_{scale}/(\sqrt{2E}2\pi\bar{d})$.

The big challenge for semiclassical methods is to calculate the large \mathcal{T} limit of $K_{uu}(\mathcal{T})$. General considerations [25] say that the form factor must approach unity as $\mathcal{T} \rightarrow \infty$. The statement is often written in terms of an explicit periodic orbit double sum analogous to (41). One should always be extremely careful when encountering such sums since they in general require regularization *even if the double sum is convergent*; otherways one will obtain an exponentially increasing form factor [27].

We will not calculate the mixed contribution K_{un} ; it may provide small corrections. It seems unlikely that K_{un} and/or K_{uu} could cancel the $1/\mathcal{T}$ decay of K_{nn} . Summing up our contributions, fig 7, we conclude that for any finite energy the form factor is not compatible with GOE for small \mathcal{T} either. The small \mathcal{T} limit governs the large scale structure of the spectrum. A convenient mesasure to study such properties is the spectral rigidity which we now will discuss.

5.3 Spectral rigidity

Spectral rigidity, or $\Delta_3(L)$ statistics [28], measures the (mean square) deviation of the spectral staircase from a linear function over L mean spacings. Small values of $\Delta_3(L)$ thus correspond to a rigid spectrum. $\Delta_3(L)$ is expressed in terms of the form factor as [25]

$$\Delta_3(L) = \frac{1}{2\pi^2} \int_0^\infty \frac{d\mathcal{T}}{\mathcal{T}^2} K(\mathcal{T})G(\pi L\mathcal{T}) \quad (45)$$

where

$$G(y) = 1 - \frac{1}{y^2} - 2\frac{\cos^2(y)}{y^2} + 6\frac{\cos(y)\sin(y)}{y^3} - 3\frac{\sin^2(y)}{y^4} \quad (46)$$

The function $G(y)$ is close to unity if $y > 1$ so for sufficiently big L the rigidity explores the small \mathcal{T} limit of the form factor.

The deviation from GOE for small \mathcal{T} implies that even if $\Delta_3(L)$ follows GOE for a while it must certainly deviate from it well before $L = 1/\mathcal{T}_{scale} = 2R\sqrt{2E}2\pi\bar{d}$. To study this we have also computed the exact quantum spectrum by the methods of ref. [17]. It is clearly seen in fig. 8 that such deviation occurs well before the saturation value L_0 corresponding to the shortest periodic orbit l_0 . Such behavior has been observed before [29]. If the form factor approaches a constant c as $\mathcal{T} \rightarrow 0$, then the rigidity will be asymptotically linearly increasing with slope $c/15$. The slope in fig. 8 is roughly 0.17 corresponding to a constant $c \approx 0.25$, which is quite compatible with the results of fig 7. As we said, we expect c to approach unity when the disk radius $R \rightarrow 0$. Accordingly the slope of Δ_3 should approach $1/15$ (as for an integrable system). That this is indeed the case is supported by the results of ref. [29].

The effect we have seen is mostly due to the neutral orbits. However, we can expect similar deviations, but perhaps less pronounced, for systems without neutral orbits. The reason is that the asymptotics of the trace (which was a slow power law for the Sinai billiard) does not set in until a length scale l_{scale} which can be much longer than the shortest periodic orbit l_0 . For instance, in the hyperbola billiard $l_0 = 1$ whereas $l_{scale} \approx 27.61$, see ref. [9].

6 Concluding remarks

We have surely not used the full potential of the methods outlined in section 3. I conclude by listing some lines along which the work may proceed.

- Improve the BER approximation by replacing the delta functions in sec 3.1 by something more realistic.
- Find corrections (similar to curvature terms) to the BER approximation. One should also correct for the nonmultiplicativity of the weight.
- Try to calculate the long \mathcal{T} limit of the form factor. It is thus essential to have good control of the fine scale structure the (properly regularized) trace $tr\mathcal{L}_{\tau=1/2}^l$. This requires that the previous two points have been worked out. Is there perhaps any simple universal structure in this fine structure?
- Work out the BER approximation (with corrections) for other systems. Each system will of course present its own problems: the stadium billiard has no natural division between a chaotic and a regular part, as it is glued together from regular components. The anisotropic Kepler problem [30] and the closed three disk billiard suffers from infinite sequences of cycles accumulating to finite length and stability. The hyperbola billiard has infinite horns.

This work was supported by the Swedish Natural Science Research Council (NFR) under contract no. F-FU 06420-303. I will also thank Predrag Cvitanović for various remarks.

Appendix

The number of coprime lattice points inside radius R in the first octant, $N_c(R)$

$$N_c(r) = \sum_{gcd(n_x, n_y)=1} \Theta(r - \sqrt{n_x^2 + n_y^2}) \quad (47)$$

is given by the integral equation

$$\frac{\pi R^2}{8} - N_c(R) = \int_0^{R/2} \frac{dN_c(r)}{dr} \left(\left\lfloor \frac{R}{r} \right\rfloor - 1 \right) dr \quad (48)$$

This equation expresses the fact that density of coprimes at radius r contributes to the density of non-coprimes at radii $2r$, $3r$ etc. Each non-coprime is uniquely related to one coprime point. This summability leads to a simple integral as above. The total number of lattice points inside radius R is $\pi R^2/8$, appearing in the left hand side. $[x]$ denotes the integral part of x , which is on the average $= x - 1/2$. Inserting this into the equation above it is easily seen that $N_c(r) = \frac{\pi}{13}r^2$ is a solution.

The introduction of maslov indices in section 4.1 motivates us to study the asymptotic behaviour of

$$\tilde{N}_c(r) = \sum_{gcd(n_x, n_y)=1} (-1)^{n_x+n_y+1} \Theta(r - \sqrt{n_x^2 + n_y^2}) \quad (49)$$

Numerical calculation suggests that $\tilde{N}_c(r) \sim 1/3 \cdot N_c(r)$. How can this be understood? The pairs (n_x, n_y) can either be (odd,odd), (odd, even), (even,odd). The (even,even) option is excluded by not being coprime. If the three possibilities have the same density the result follows.

References

- [1] W. Zurek, *this volume*.
- [2] O. Bohigas, M. J. Giannoni and C. Schmit, Phys. Rev. Lett. **52**, 1 (1984).
- [3] M. C. Gutzwiller, *Chaos in Classical and Quantum Mechanics*, Springer, New York (1990).
- [4] A. Voros, J. Phys. A **21**, 685 (1988).
- [5] P. Cvitanović and B. Eckhardt, J. Phys. A **24**, L237 (1991).
- [6] P. Cvitanović, P.E. Rosenqvist, H.H. Rugh and G. Vattay, Chaos **3**, 619 (1993).
- [7] P. Cvitanović and P.E. Rosenqvist, in G.F. Dell'Antonio, S. Fantoni and V.R. Manfredi, eds., *From Classical to Quantum Chaos, Soc. Italiana di Fisica Conf. Proceed.* **41**, pp. 57-64 (Ed. Compositori, Bologna 1993).
- [8] R. Artuso, E. Aurell and P. Cvitanović, Nonlinearity **3**, 325; **3** 361, (1990).
- [9] P. Dahlqvist, J. Phys. A **27**, 763 (1994).
- [10] P. Cvitanović and G. Vattay, Phys. Rev. Lett. **71**, 4138 (1993).
- [11] C. Beck, F. Schlögl, *Thermodynamics of chaotic systems*, Cambridge Nonlinear Science Series 4, Cambridge (1993).
- [12] H. H. Rugh, Nonlinearity **5**, 1237 (1992).
- [13] V. Baladi, J. P. Eckmann and D. Ruelle, Nonlinearity **2**, 119 (1989).
- [14] Y. G. Sinai, Russ. Math. Surv. **25**, 137 (1979).
- [15] P. Dahlqvist, *Approximate zeta functions for the Sinai billiard and related systems*, submitted to Nonlinearity.
- [16] P. Cvitanović and B. Eckhardt, Nonlinearity **6**, 277 (1993).
- [17] M. V. Berry, Ann. Phys. (N.Y.) **131**, 163 (1981).
- [18] H. Rademacher, *Lectures on Elementary Number Theory*, Blaisdell Publishing Company, New York.
- [19] P. Cvitanović, *this volume*.
- [20] B. Sundaram, *this volume*.
- [21] M. V. Berry and J. K. Keating, J. Phys. A **23**, 4839 (1990).
- [22] M. Sieber and F. Steiner, Phys. Rev. Lett. **67**, 1941 (1991).

- [23] S. C. Creagh and R. G. Littlejohn, Phys. Rev. A **44**, 836, (1991).
- [24] M. V. Berry and M. Tabor, Proc. R. Soc. Lond. A **356**, 375 (1977).
- [25] M. V. Berry, Proc. R. Soc. Lond. A **400**, 229 (1985).
- [26] M. L. Mehta, *Random matrices and the statistical theory of energy levels*, Academic Press, New York (1967).
- [27] R. Aurich and M. Sieber, J. Phys. A **27**, 1967 (1994).
- [28] F. J. Dyson and M. L. Mehta, J. Math. Phys. **4**, 701 (1963).
- [29] P. Arve, Phys. Rev. A **44**, 6920 (1991).
- [30] G. Tanner and D. Wintgen, *Classical and Semiclassical Zeta Functions in Terms of Transition Probabilities*, to appear in "Chaos, Solitons and Fractals".